Matsushita, E. *et al*., Supplemental Material

Legends for Supplemental Figures

Supplemental Figure S1. Expression profile of Gipie

(A) Tissue distribution of Gipie in postnatal (P2) and adult (P56) mice. Using specific primers for Gipie and β-actin, RT-PCR shows the ubiquitous expression of Gipie in mice. **(B)** Expression of Gipie in primary endothelial cells and cell lines derived from macrophages. HCAEC, human coronary artery endothelial cells; HUVEC, human umbilical vein endothelial cells; COS-7, SV40 transformed African Green monkey kidney cells; U937, human histiocytic lymphoma; THP-1, human monocytic leukemia; HEK293, human embryonic kidney cells; HeLa, human cervical adenocarcinoma; HT1060 human fibrosarcoma; A549; human lung squamous cell carcinoma; DLD-1, human colon adenocarcinoma, SW480; human colon adenocarcinoma; TGW, human neuroblastoma; HL-60, human promyelocytic leukemia; Raji, human Burkitt lymphoma; MC, SK-N-MC human neuroblastoma.

Supplemental Figure S2. Lack of detectable interaction between endogenous Gipie and PDI

Lysates from HUVECs were immunoprecipitated (IP) with anti-Gipie, anti-PDI, or normal rabbit IgG antibody, followed by Western blot analysis using anti-PDI (left panel) or anti-Gipie (right panel) antibodies. No apparent interaction between Gipie and PDI was found.

Supplemental Figure S3. Girdin and Daple, members of the Girdin family of proteins, fail to interact with GRP78, and are not involved in the thapsigargin-induced UPR pathway

(A) Lysates from HUVECs were immunoprecipitated (IP) with anti-GRP78 or normal rabbit IgG antibody, followed by Western blot analysis using the indicated antibodies. Girdin and Daple did not interact with GRP78 under our experimental conditions. **(B)** HUVECs were incubated with 0.5 or 1 μmol/L thapsigargin (TG) for eight hr. Total cell lysates were subjected to Western blot analysis with the indicated antibodies. **(C)** Expression levels of Girdin (upper panel) and Daple (lower panel) shown in **(B)** were quantified by densitometric scanning. The values are presented as the fold-increase in expression relative to the control.

Supplemental Figure S4. Gipie regulates the interaction between GRP78 and IRE1 as well as ER stress-induced apoptosis in COS7 cells

(A) Gipie suppressed the ER stress-induced phosphorylation of JNK, but not that of elF2α. Non-transfected (control) COS7 cells or cells transfected with either Gipie or V5 empty vector were treated with 1 μmol/L TG for eight hr, and total cell lysates were subjected to Western blot analysis using the indicated antibodies. **(B)** Regulation of GRP78 interaction with IRE1 by Gipie. Total cell lysates and GRP78 immunoprecipitates from non-transfected COS7 cells or cells transfected with either Gipie or V5 empty vector were subjected to Western blot analysis using the indicated antibodies. Note that the amount of IRE1 detected in the GRP78 immunoprecipitates was increased by the transfection of Gipie (asterisk). In the right panels, the amounts of IRE1, ATF6, and PERK detected in the GRP78 immunoprecipitates shown in the left panels were quantified by densitometric scanning, and the values are presented as the

fold-increase in expression relative to the control (*P < 0.05; **not significant (N.S.)). **(C)** Effects of Gipie on ER stress-induced expression of CHOP. COS7 cells were transfected with either Gipie or V5 empty vector and were subsequently treated with 1 μmol/L thapsigargin for eight hr. Total cell lysates were analysed by Western blotting using anti-CHOP antibody. In the lower panel, the amounts of CHOP were quantified by densitometric scanning, and the values are presented as the fold-increase in expression relative to the control. An asterisk indicates significant difference (*P < 0.05). **(D)** Effects of Gipie on ER stress-induced apoptosis. COS7 cells transfected with either Gipie or V5 empty vector were incubated with 1 μmol/L TG for eight hr, followed by annexin V staining (green) to detect apoptotic cells. In the right panel, the percentage of annexin V-positive cells was quantified. An asterisk indicates a statistically significant difference (*P < 0.05, *t*-test).

Supplemental Figure S5. Exogenously expressed Gipie had no significant effect on the degradation of IRE1

(A) 293FT cells were transfected with either the IRE1β-HaloTag vector or control empty vector. Lysates were subjected to Western blot analysis using anti-HaloTag antibody. **(B)** HeLa cells were transfected with either the IRE1-Halo vector or control vector and were incubated with 5 μmol/L HaloTag TMR (tetramethylrhodamine) ligand for ten min. After washing, fluorescence microscopy showed the expression of IRE1β-HaloTag in the ER (red). Nuclei were visualized by DAPI (blue). Scale bar: 10 μm. **(C)** IRE1β-HaloTag was pulse-labeled with TMR ligand and chased at indicated time intervals in the presence or the absence of MG132 (10 μM) in Gipie-V5-transfected or control COS7 cells. Expression levels of Gipie-V5 were monitored by Western blot analysis. The expression of Gipie had no apparent effects on the degradation of IRE1.

Supplemental Figure S6. Anti-apoptotic effects of Gipie are mediated by its interaction with GRP78

(A) Effects of Gipie and its mutants on ER stress-induced expression of CHOP. COS7 cells transfected with the indicated plasmid vectors (see Figure 3C) were treated with 1 μmol/L TG for eight hr, and the expression of CHOP was analysed by Western blot analysis. **(B)** The amounts of CHOP shown in **(A)** were quantified by densitometric scanning, and the values are presented as fold-increases in expression relative to the control. An asterisk indicates a statistically significant difference (*P < 0.05; N.S., not significant). **(C)** Effects of Gipie and its mutants on ER stress-induced apoptosis. COS7 cells transfected with the indicated plasmid vectors were incubated with 1 μmol/L TG for eight hr, followed by annexin V staining (green) to detect apoptotic cells. **(D)** Percentages of annexin V-positive cells shown in **(C)** were quantified. An asterisk indicates statistically significant difference (*P < 0.05; N.S., not significant).

Supplemental Figure S7. Expression of Gipie in nascent endothelial cells and neointima after balloon injury

(A) Paraffin-embedded sections from rat carotid arteries six weeks after balloon injury were stained with anti-Gipie (green) and anti-PECAM1 (red) antibodies. Nuclei were visualized with DAPI staining (blue). The regions within the white boxes (a and b) are shown at higher magnifications in lower panels. Arrowheads in a and arrows in b indicate the expression of Gipie in nascent endothelial cells generated during the process of restenosis. **(B)** Paraffin-embedded sections from rat carotid arteries six weeks after balloon injury were stained with anti-Gipie (green), anti-α-smooth muscle actin (red) antibodies, and DAPI (blue). Note that Gipie expression was significantly

increased in endothelial cells and neointima of the artery after the balloon injury (lower panels). Three rats were analyzed in each group. Scale bars: 200μm.

Supplemental Figure S8. Cyclic mechanical stretching had no significant effect on Gipie expression in HUVECs

HUVECs were cultured on fibronectin-coated silicon chambers and subjected to uniaxial cyclic mechanical stretch (30 cycles/min; 0.5 sec stretching, 1.5 sec relaxation; 15% elongation). Total cell lysates were analyzed by Western blotting with the indicated antibodies. Cyclic mechanical stretch had no significant effect on the expression of either Gipie or GRP78 under the experimental conditions.

Supplemental Figure S9. No apparent effect of Gipie on splicing of the transcription factor XBP-1

COS7 cells **(A)** and HUVECs **(B)** transfected with either Gipie or V5 empty vector, or HUVECs transfected with either Gipie or control siRNA **(C)** were incubated with 1 μmol/L TG for eight hr. Total RNA was harvested immediately after TG treatment and subjected to RT-PCR analysis. Expression levels of Gipie were monitored by Western blot analysis. Primers spanning the splice junction in XBP-1 were used to amplify the products of unspliced and spliced mRNA. RT-PCR analysis of untreated cells detected a single band corresponding to unspliced mRNA. By contrast, both unspliced and spliced XBP-1 mRNAs were detected in cells treated with TG. The amounts of spliced XBP-1 mRNA in Gipie-expressing and Gipie knock down cells were comparable to that in control cells.

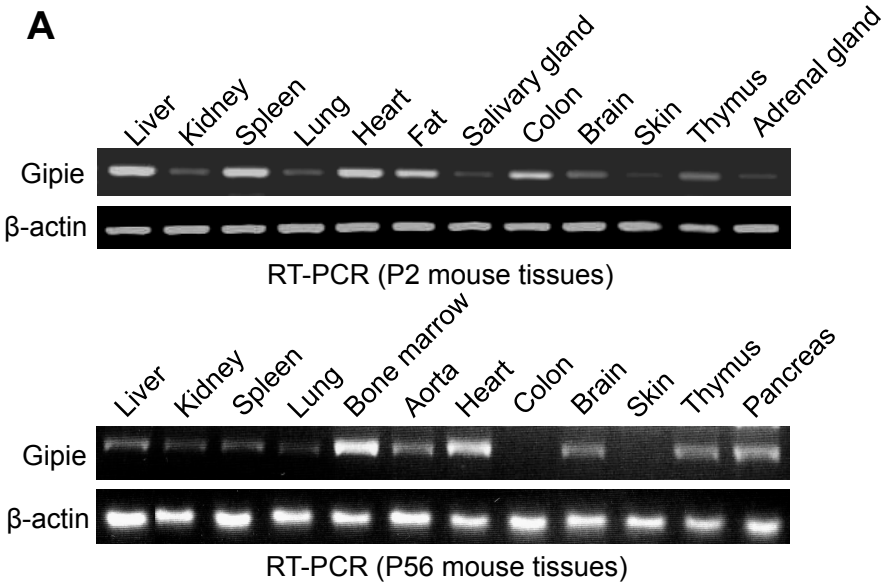

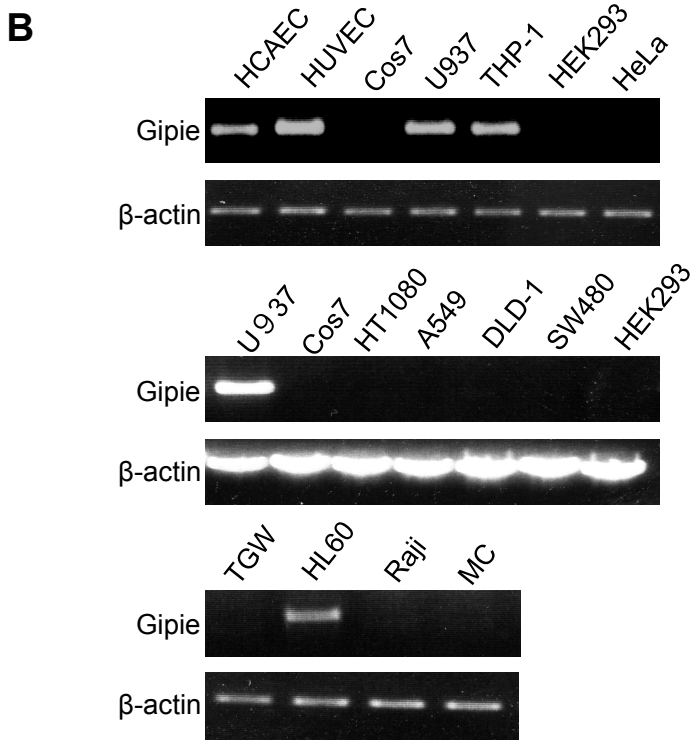

Suppl. Fig. S1, Matsushita et al.

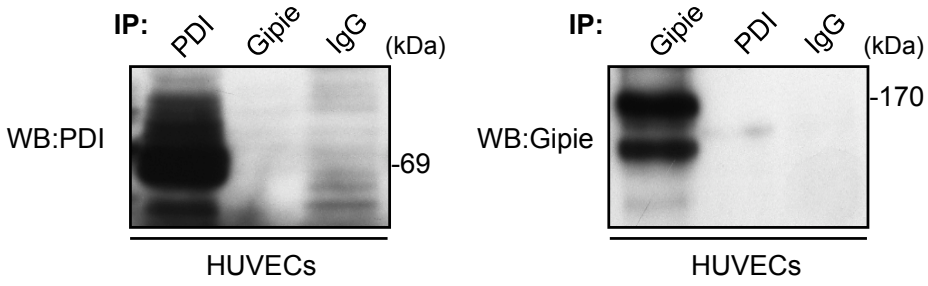

Suppl. Fig. S2, Matsushita et al.

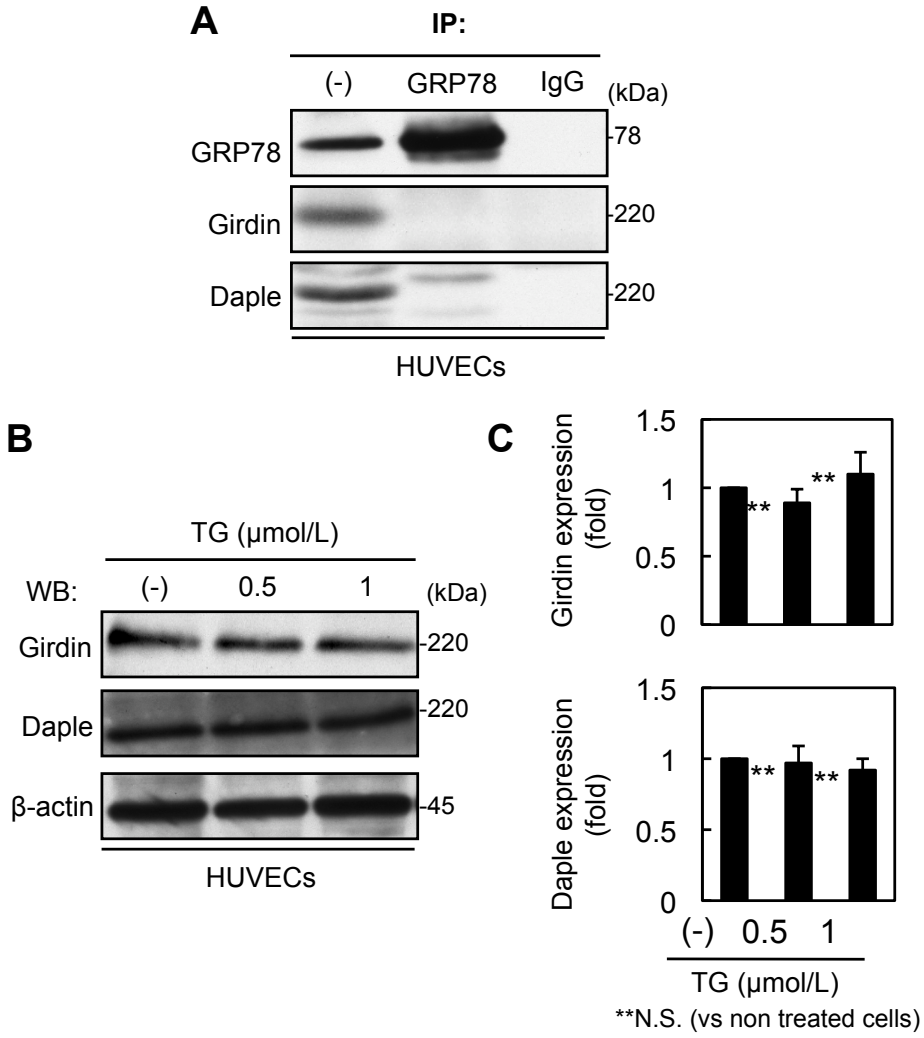

Suppl. Fig. S3, Matsushita et al.

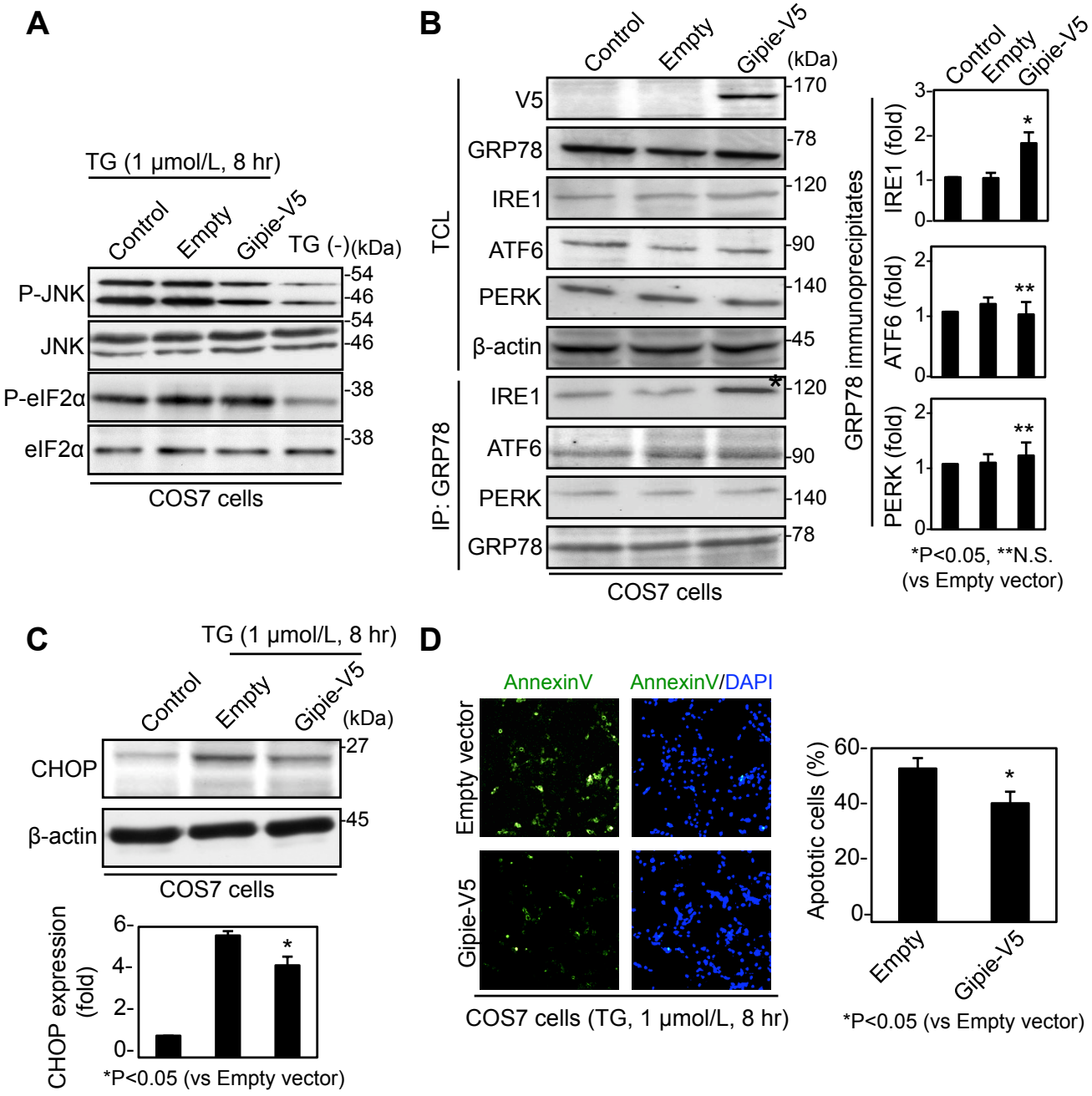

Suppl. Fig. S4, Matsushita et al.

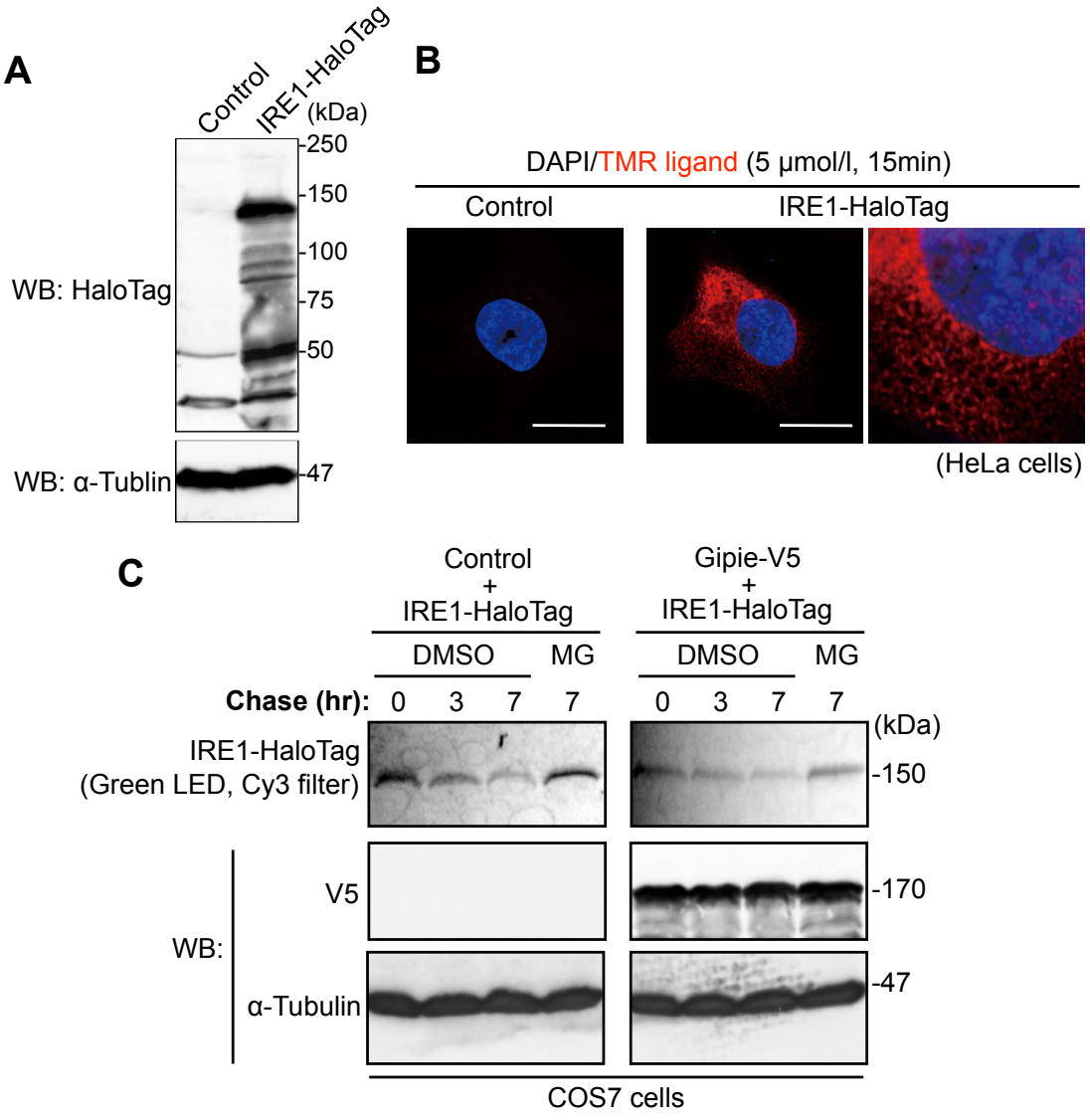

Suppl. Fig. S5, Matsushita et al.

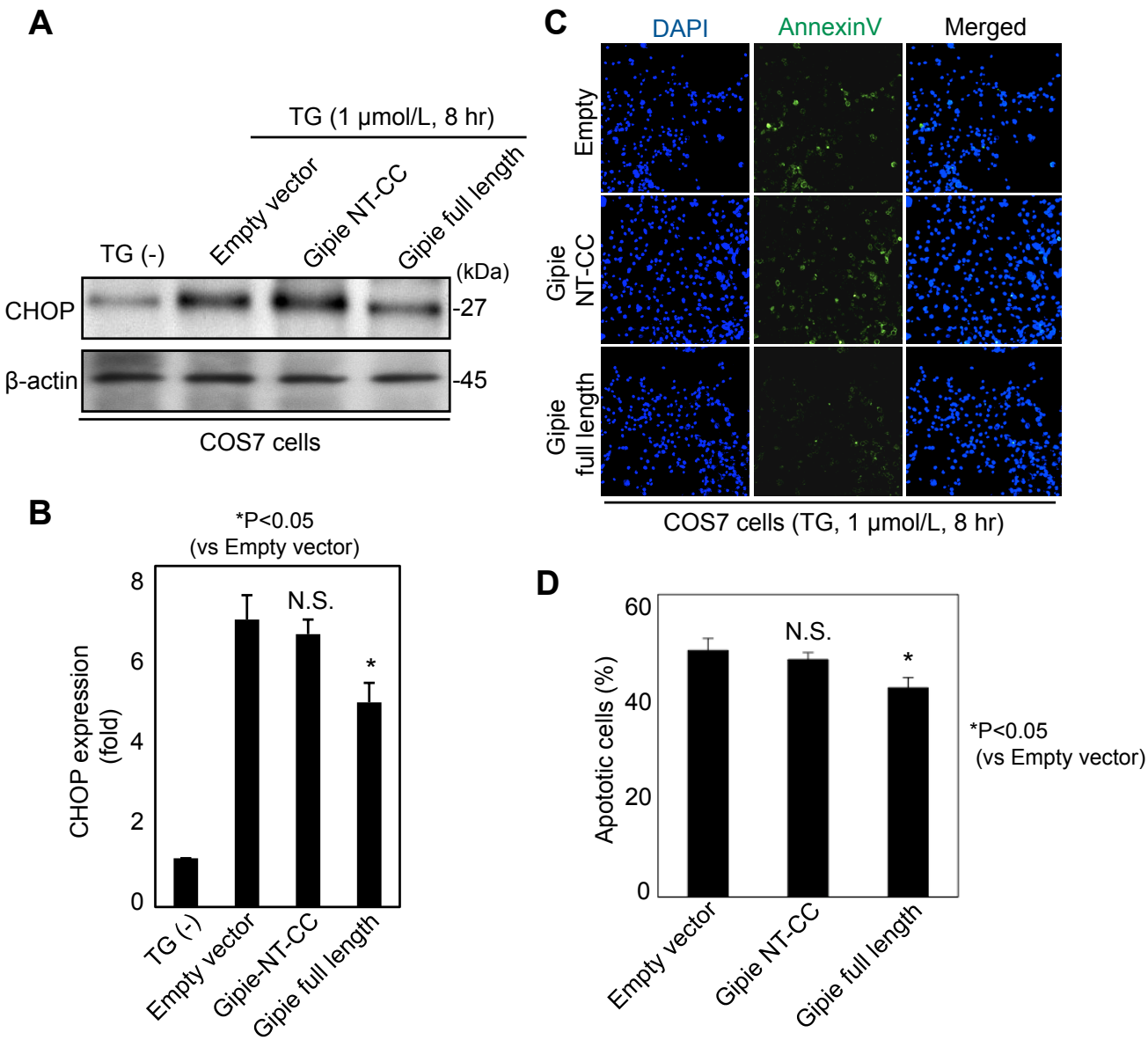

Suppl. Fig. S6, Matsushita et al.

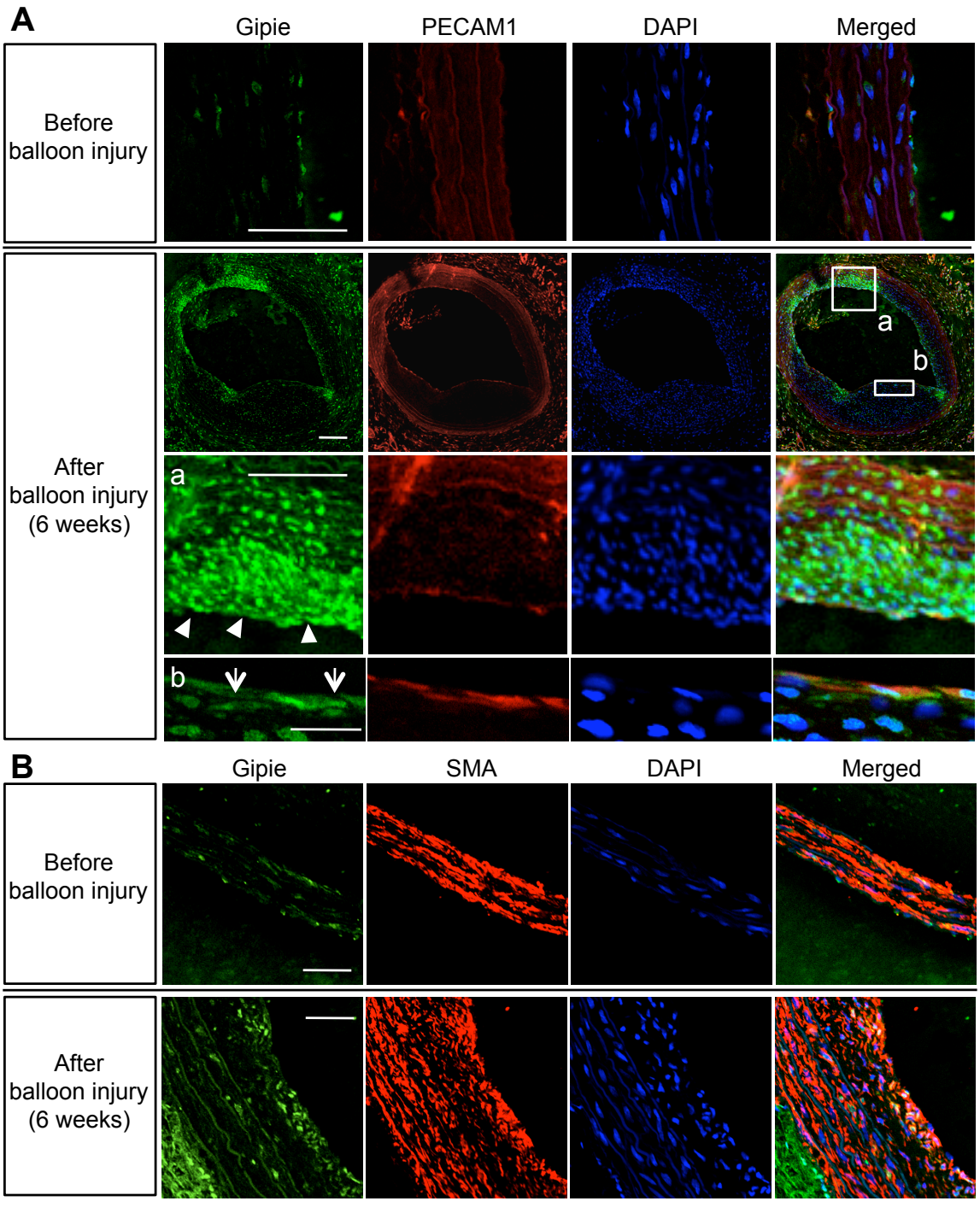

Suppl. Fig. S7, Matsushita et al.

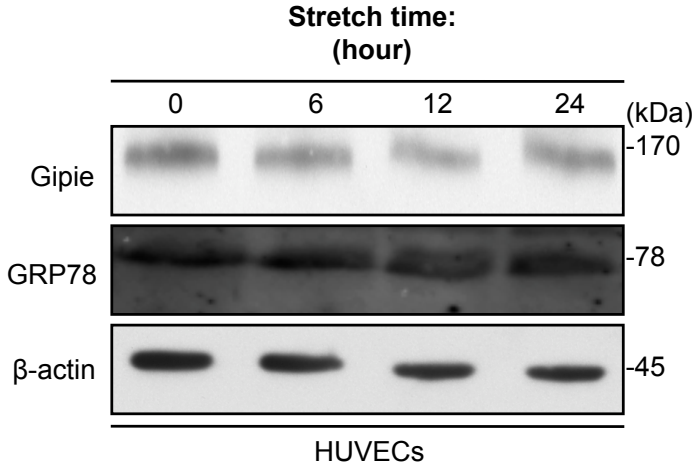

Suppl. Fig. S8, Matsushita et al.

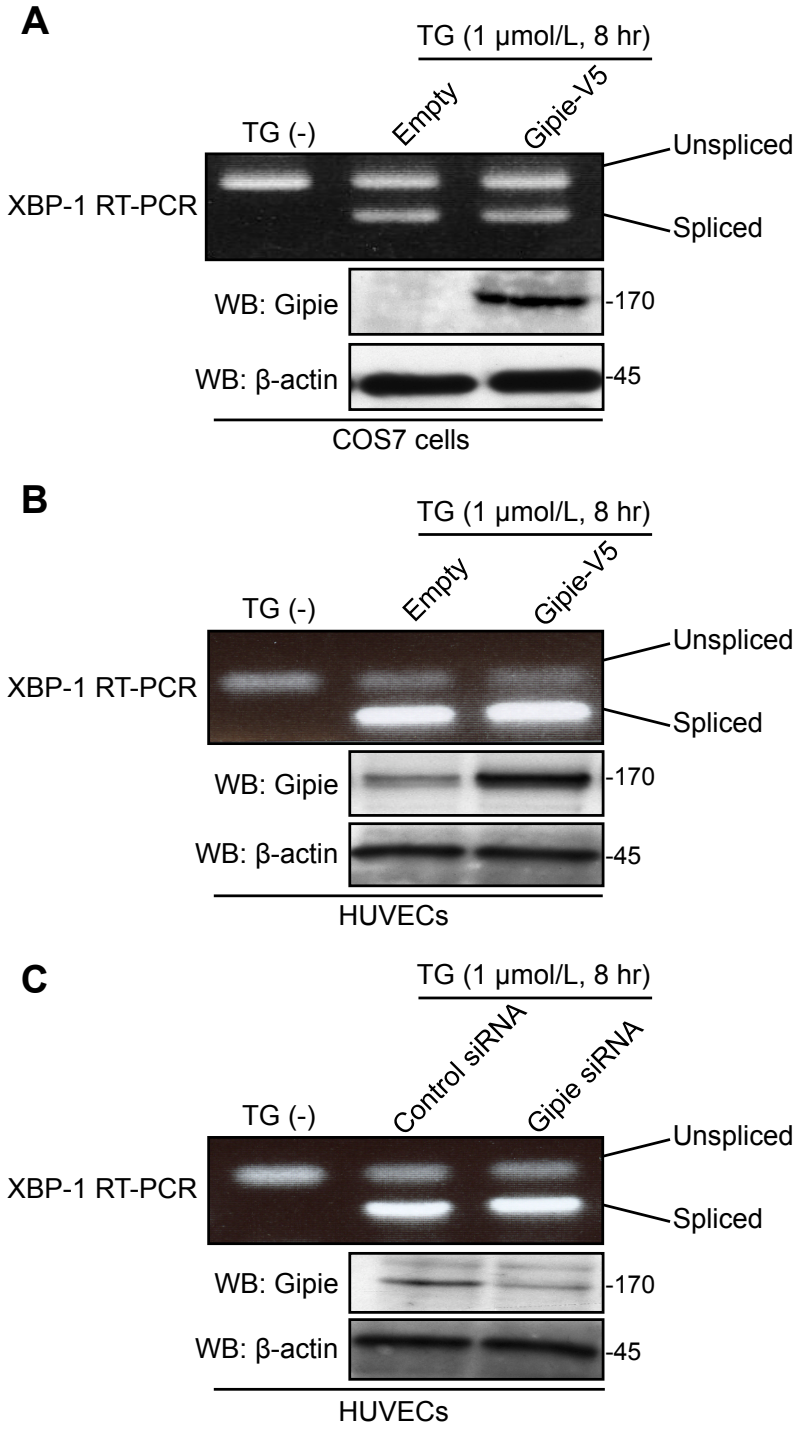

Suppl. Fig. S9, Matsushita et al.